

He, W., Lin, T., Song, Z., Cheng, Y., Zheng, R., Chen, W., [Miras, H. N.](#) and Song, Y.-F. (2023) Fabrication of epitaxially grown  $\text{Mg}_2\text{Al-LDH}$ -modified nanofiber membranes for efficient and sustainable separation of water-in-oil emulsion. *ACS Applied Materials and Interfaces*, 15(3), pp. 4755-4763. (doi: [10.1021/acsami.2c19015](https://doi.org/10.1021/acsami.2c19015))

This is the author version of the work. There may be differences between this version and the published version. You are advised to consult the published version if you wish to cite from it:

<https://doi.org/10.1021/acsami.2c19015>

Copyright © 2023 American Chemical Society

<https://eprints.gla.ac.uk/289963/>

Deposited on 17 February 2023

Enlighten – Research publications by members of the University of Glasgow  
<http://eprints.gla.ac.uk>

# **Fabrication of Epitaxially Grown Mg<sub>2</sub>Al-LDH Modified Nanofiber Membranes for Efficient and Sustainable Separation of Water-in-Oil Emulsion**

Wenjun He, <sup>a†</sup> Tong Lin, <sup>a†</sup> Ziheng Song, <sup>a</sup> Yao Cheng, <sup>a</sup> Ruoxuan Zheng, <sup>a</sup> Wei Chen,  
<sup>a\*</sup> Haralampos N. Miras, <sup>b\*</sup> and Yu-Fei Song <sup>a\*</sup>

<sup>a</sup>State Key Laboratory of Chemical Resource Engineering, Beijing University of Chemical Technology, Beijing 100029 P. R. China. \*E-mail: chenw@mail.buct.edu.cn, songyf@mail.buct.edu.cn; Fax/Tel: +86 10-64431832;

<sup>b</sup>WestCHEM, School of Chemistry, University of Glasgow, Glasgow, G12 8QQ, UK. \*E-mail: charalampos.moiras@glasgow.ac.uk.

<sup>†</sup>These authors contributed equally on this work.

**Abstract:** Efficient separation of the water-in-oil emulsion is of great importance but remains highly challenging since such emulsion contains stable tiny size droplets with diameter less than 20  $\mu\text{m}$ . Herein, we reported the fabrication of a modular fibrous functional membrane using “*in-situ* growth and covalent functionalization” strategy. The as-prepared PAN@LDH@OTS (PAN = polyacrylonitrile; LDH = layered double hydroxides; OTS = octadecyltrichlorosilane) membrane possessed an interlaced rough nanostructured surface with intriguing superhydrophobic/superlipophilic properties. When applied for the separation of surfactant-stabilized water-in-oil emulsion (SSE), the PAN@LDH@OTS membrane exhibited an ultrahigh permeation flux of up to  $4.63 \times 10^4 \text{ L m}^{-2} \text{ h}^{-1}$  with an outstanding separation efficiency of  $> 99.92\%$ , outperforming most of the state-of-the-art membranes. Besides, the membrane can maintain a stable permeation flux and the superhydrophobic/superlipophilic properties after 20 times use. Detailed characterization demonstrated that the demulsification of SSE process was as following: Firstly, the droplets can be easily adsorbed to the PAN@LDH@OTS membrane due to the improved intermolecular interactions between OTS and the surfactants (Span-80); Secondly, the droplets can be deformed by the electropositive LDH laminate; Thirdly, the deformed tiny emulsion droplets coalesced into large droplets, floated up and as a result, efficient separation of SSE can be achieved.

**Keywords:** Polyacrylonitrile; Layered double hydroxides; Surfactant; Superhydrophobic/superlipophilic surface; Emulsion.

## Introduction

The increasing release of industrial oil-based wastewater as well as frequent crude oil leakage has a serious impact on marine ecological environment. For example, in the Penglai oil spill in China 2011, there were about 700 barrels of crude oil leaking into the Bohai Sea, which caused 2,500 barrels of oil-based drilling fluid (mainly containing water-in-oil emulsion) to leak and deposit on the seabed. To deal with such oily wastewater and water-in-oil emulsion discharge, huge amounts of economic loss is consumed, but serious ecological and environmental pollution still exists.<sup>1, 2</sup> More importantly, the separation of the water-in-oil emulsion, which contains a large number of stable tiny water droplets with diameters of less than 20  $\mu\text{m}$ , is challenging by using current separation technologies including mechanical separation and centrifugation.<sup>3</sup> Therefore, it is necessary to develop viable solutions for effective separation of water-in-oil emulsion.

As a low cost, small footprint and easy for continuous operation material for separation and purification, the superhydrophobic/superlipophilic membranes possess unique properties such as self-cleaning, antifouling and energy-saving fluid transmission, and have attracted widespread attention in the separation of water-in-oil emulsion.<sup>4-8</sup> For example, Jiang *et al.*<sup>9</sup> reported a superhydrophobic polytetrafluoroethylene coated stainless steel mesh for gravity driven oil-water separation. Since then, the interfacial super-wetting membrane with a pore size-sieving effect was applied for separation of water-in-oil emulsion. Zhao *et al.*<sup>10</sup> designed an integrated a fluor silane nano-needle superhydrophobic membrane, achieving high-flux, high-efficiency and continuous oil/water separation. Li *et al.* designed biomass<sup>11</sup>, organic<sup>12</sup>, inorganic<sup>13</sup> and other porous membranes, which achieved various emulsion separation as well as dye and heavy metal ion adsorption. Cheng *et al.*<sup>14</sup> fabricated a flexible superhydrophobic membrane by surface self-assembly and subsequent thiol modification, and the resultant hierarchical nanofibrous membrane can be applied for separating oil/water mixtures with a permeation flux of over 2000  $\text{L m}^{-2} \text{h}^{-1}$ . Shao *et al.*<sup>4</sup> prepared a superhydrophobic membrane with a unique hierarchical chemical structure

and micro-nanoscale morphology structure, which can resist physical abrasion. Currently, since the nanofibrous membranes for oily water purification is still in its infancy, there are many challenges to be addressed. For example, most hierarchical structures are not stable enough and can be easily destroyed by external force, resulting in the decrease and/or loss of separation function of the nanofibrous membrane.<sup>15</sup> Moreover, the membrane permeation flux and separation efficiency need to be further improved. In order to improve separation efficiency for water-in-oil emulsion with diameters less than 20  $\mu\text{m}$ , the membrane should have the following structural characteristics: 1) the membrane has a stable superhydrophobic structure so that water cannot infiltrate the membrane to realize the selective separation; 2) the membrane has high porosity and permeability to achieve high permeability flux; 3) multiple interactions between the components of membrane and emulsion droplets can enhance effective contact and realize rapid demulsification.

Herein, we successfully fabricated the PAN@LDH@OTS membrane by “*in-situ* growth and covalent functionalization” strategy (PAN = polyacrylonitrile; LDH = layered double hydroxides; OTS = octadecyltrichlorosilane). The as-prepared PAN@LDH@OTS membrane combined the advantages of hierarchical roughness and sub-micron pore structure and showed superhydrophobic/superlipophilic properties. The pores formed by stacked PAN fibers increased the contact area between the emulsion droplets and the membrane, which significantly improved permeation flux. Moreover, the electropositive LDH laminate promoted the deformation of the emulsion droplets. More importantly, the covalent modification of OTS effectively reduced the surface free energy of the PAN@LDH and the resultant PAN@LDH@OTS showed strong interface interactions with the surfactants of SSE droplets. As a result, efficient, stable and durable SSE separation by the PAN@LDH@OTS membrane can be achieved.

## Result and Discussion

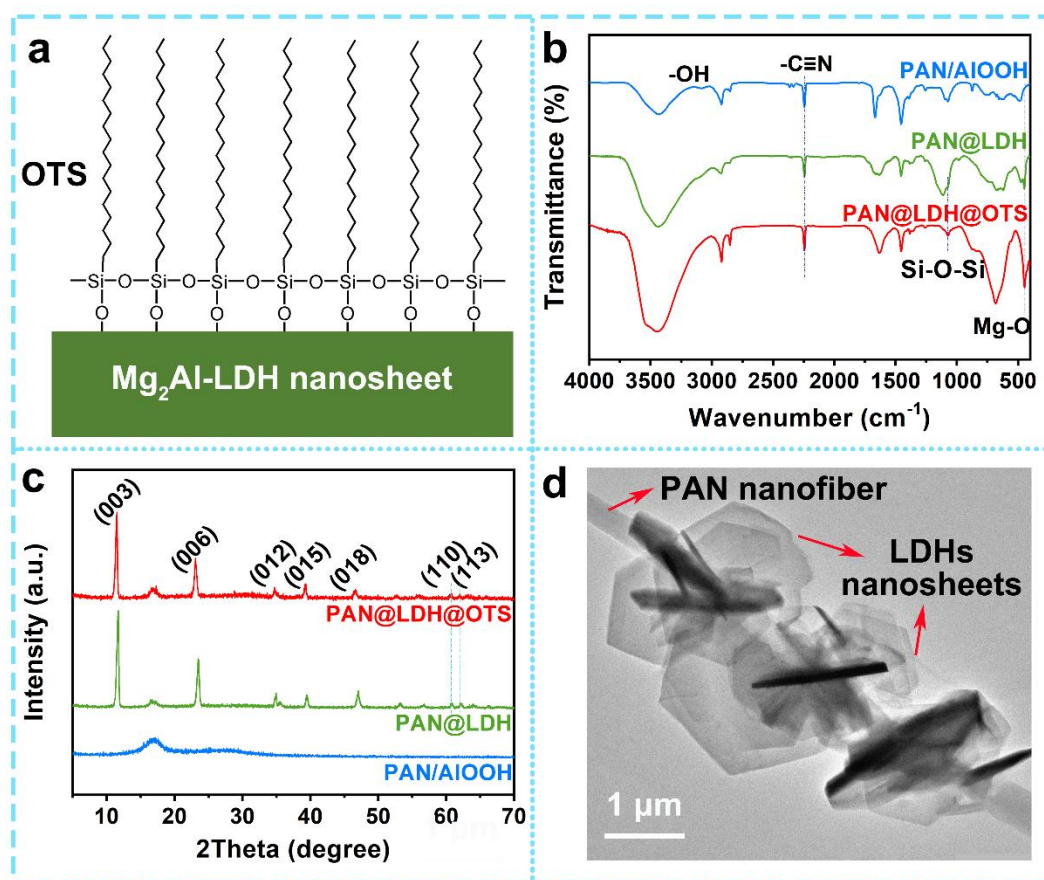


**Figure 1.** a) Schematic representation of the molecular structure of LDH laminate after covalent functionalization of OTS, b) FT-IR spectra and c) XRD patterns of PAN/AIOOH, PAN@LDH, and PAN@LDH@OTS membranes, respectively, d) TEM image of the PAN@LDH@OTS membrane.

The PAN/AIOOH membrane were fabricated by the electrospinning method, and  $\text{MgAl-LDH}$  plates were grown on PAN fibers by using AIOOH as aluminium source and adopting hydrothermal method<sup>16-18</sup>. After that, OTS was covalently modified on PAN@LDH membrane (Figure 1a and Figure S1). Each step was characterized by Fourier transform infrared (FT-IR) spectra (Figure 1b) and X-ray diffraction (XRD) patterns (Figure 1c). As shown in Figure 1b, after *in-situ* growth of the LDH, the PAN@LDH membrane displayed prominent peaks at 784, 685 and 447  $\text{cm}^{-1}$ , which can be assigned to the Mg-O-Al, Mg-OH-Al and Mg-O stretching vibrations, respectively. For PAN@LDH@OTS, FT-IR showed the characteristic absorption peaks

of both LDH and PAN. For example, the characteristic stretching vibration of the  $\text{-C}\equiv\text{N}$  bond of PAN can be observed at  $2244\text{ cm}^{-1}$ , along with the  $\text{-CH}_2\text{-}$  vibration at  $2920$  and  $2851\text{ cm}^{-1}$ . In addition, new peaks at  $1060\text{ cm}^{-1}$  and in the region of  $890\sim 690\text{ cm}^{-1}$  (Figure 1b) were corresponded to the Si-O-M (M = Mg, Al) and Si-C bonds,<sup>19</sup> confirming that the OTS was successfully modified. As shown in Figure 1d, XRD pattern of the PAN/AlOOH exhibited a strong reflection peak centred at  $2\theta = 17.1^\circ$ , which was attributed to the hexagonal crystal (010) plane of the PAN.<sup>20</sup> For PAN@LDH, the characteristic diffraction peaks at  $2\theta = 11.7, 23.6, 35.0, 39.6, 47.1, 60.9$  and  $62.1^\circ$  due to the (003), (006), (012), (015), (018), (110) and (113) planes of LDH can be observed.<sup>21</sup> For PAN@LDH@OTS, XRD diffraction retained its layered structure of LDH with the reflection peaks of (003) and (006) planes at  $11.7$  and  $62.1^\circ$ , respectively. Transmission Electron Microscope (TEM) image of PAN/LDH showed that the LDH microcrystals with their characteristic hexagonal plate-like morphology were aligned vertically, and nanofibers packed densely (Figure 1d).<sup>18</sup> It should be noted that the morphology of the PAN@LDH@OTS displayed no obvious change, compared with that of PAN@LDH (Figure S2). AFM results indicated the surface roughness of PAN@LDH@OTS was  $170\text{ nm}$ . (Figure S3)

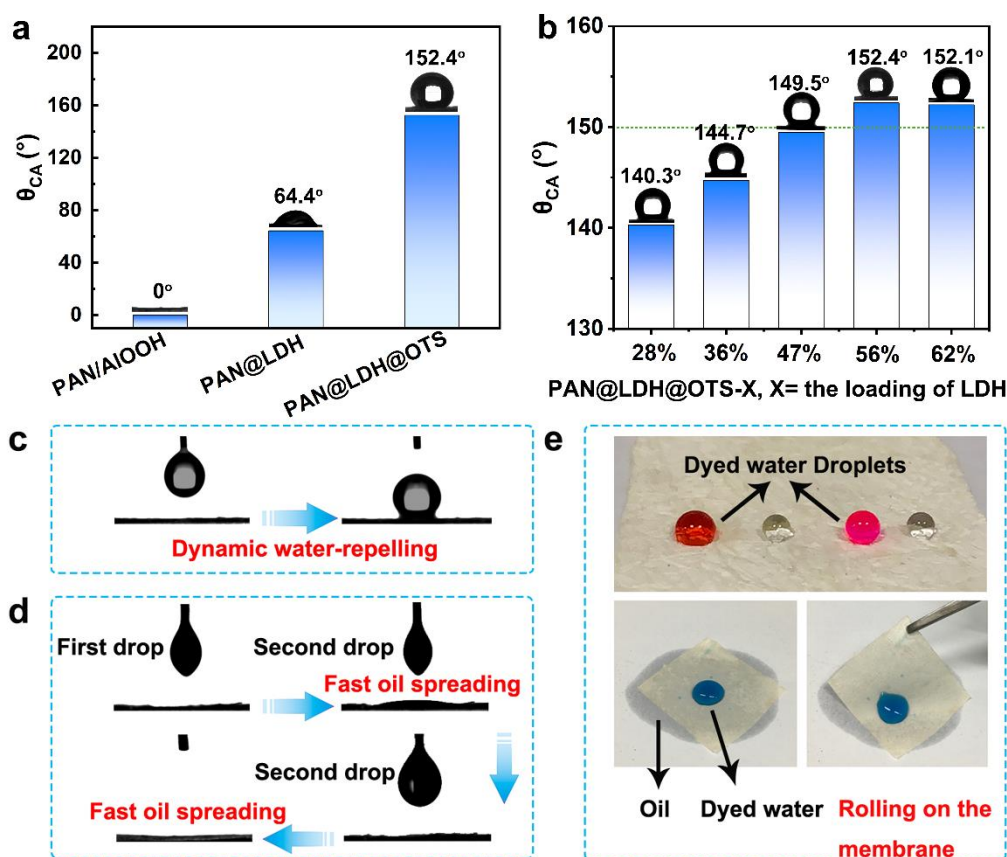


**Figure 2. Superhydrophobic/superlipophilic properties:** a) Water contact angle ( $\theta_{CA}$ ) of PAN/AIOOH, PAN@LDH and PAN@LDH@OTS membranes, respectively. b) Water contact angle ( $\theta_{CA}$ ) with different LDH loading of the modified membranes (PAN@LDH@OTS-X correspond to PAN@LDH@OTS-28%, PAN@LDH@OTS-36%, PAN@LDH@OTS-47%, PAN@LDH@OTS-56% and PAN@LDH@OTS-62% membrane, respectively. The percentages represent different loading of LDH.). Photographs of dynamic measurements of c) water rejection and d) oil spreading on the surface of PAN@LDH@OTS membrane. e) Photograph showing the superhydrophobic and superlipophilic of the membrane towards water (dyed red, pink and blue) in air.

Surface wettability was a critical factor to evaluate the membrane properties because it can affect the liquid permeate as well as foulants resistance. Therefore, we tested the contact angle between the droplet and the membrane's surface to investigate the waterproof properties of the membranes. As shown in Figure 2a, the PAN/AIOOH and PAN@LDH membranes exhibited the  $\theta_{CA}$  (water contact angle) of 0° and 64.4°, respectively. In contrast, after covalent modification with OTS, the PAN@LDH@OTS



membrane revealed an impressive  $\theta_{CA}$  value of  $152.4^\circ$ , which was indicative of its superhydrophobic properties. To investigate the effect of the LDH loadings on the  $\theta_{CA}$  of PAN@LDH@OTS membrane, we tested four samples with different LDH loadings ranging from 28 to 62% (Figure 2b and Figure S4). Obviously, the membrane with LDH loading of 56% and 62% presented the  $\theta_{CA}$  of  $152.4^\circ$  and  $152.1^\circ$ , respectively, indicating the best superhydrophobicity. Considering that the PAN@LDH@OTS membrane can still maintain superhydrophobicity with the increase of LDH loading when the LDH loading of PAN@LDH@OTS membrane was higher than 56%, therefore, the subsequent investigation of the efficiency in separation processes was focused on the superhydrophobic PAN@LDH@OTS-56% membrane (denoted as PAN@LDH@OTS).

The PAN@LDH@OTS membrane showed low adhesion to water (Figure 2c) since the water droplet can recede completely from the membrane without spreading. In contrast, oil can spread rapidly on the surface of PAN@LDH@OTS membrane in only about 3s (Figure 2d) due to the superhydrophobic/superlipophilic properties of the membrane. When the dyed water droplets were added to the PAN@LDH@OTS membrane (Figure 2e), the spherical water droplets remained its morphology. After fully wetting the PAN@LDH@OTS membrane with oil, the dyed water droplets can slide freely on the surface of the membrane. All these results proved the superhydrophobicity of the PAN@LDH@OTS membrane

The oil adsorption capacity of PAN@LDH@OTS membrane was evaluated by a combination of qualitative and quantitative measurements, providing better understanding of the adsorption behaviour of the membrane. The  $\text{CH}_2\text{Cl}_2$  was used as the model oil due to its density was higher than the water. When the membrane contacted with the oily phase in water, the oil was absorbed rapidly ( $\sim 10$  s) (Figure 3a). Besides, the adsorption capacity of the PAN@LDH@OTS membrane toward 6 different types of oil and/or organic solvents were conducted (Figure 3b). The results showed that the PAN@LDH@OTS membrane was capable to absorb 20-35 times oils than its own weight.

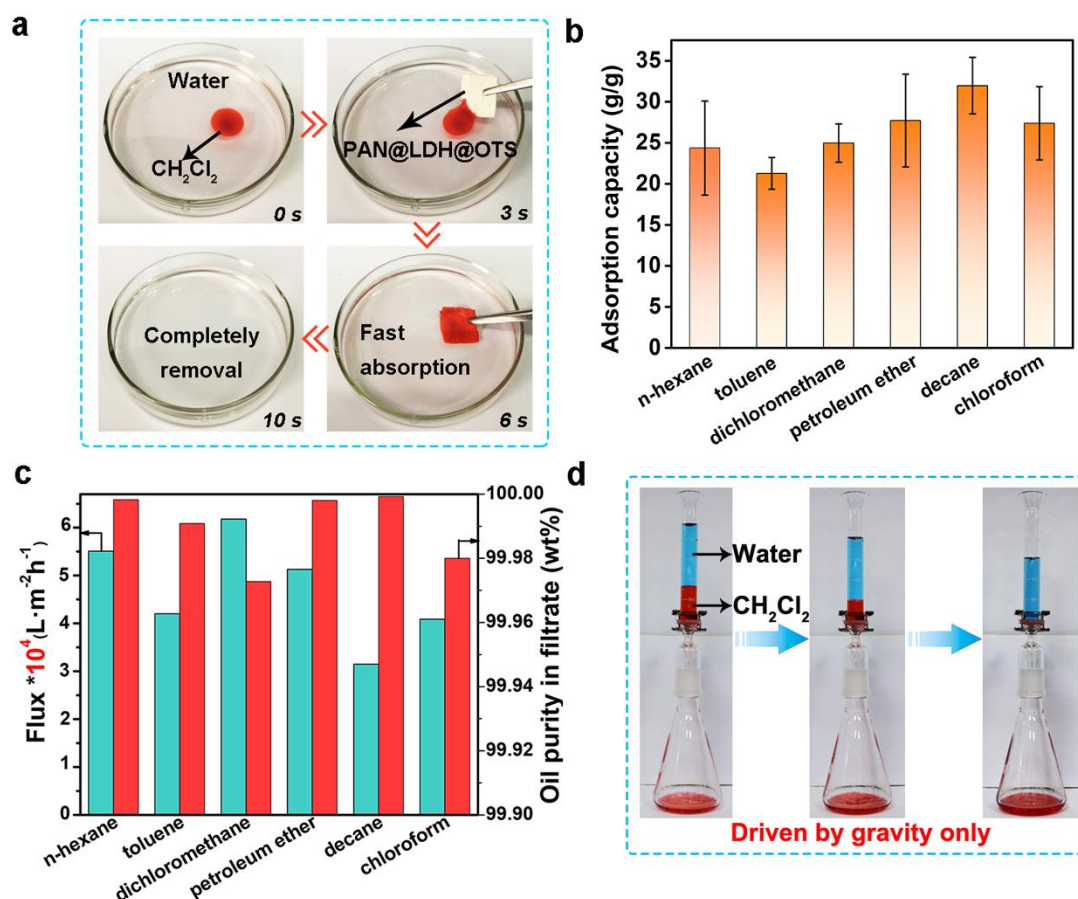


**Figure 3. Separation of oil/water mixture:** a) Photographs showing the collection of CH<sub>2</sub>Cl<sub>2</sub> floating on the water surface with the PAN@LDH@OTS membrane; b) PAN@LDH@OTS membrane's oil absorption ability test for the six oils used for this study (n-hexane, toluene, dichloromethane, petroleum ether, decane and chloroform); c) Water/oil mixture separation results of the PAN@LDH@OTS membrane; d) The CH<sub>2</sub>Cl<sub>2</sub>/water separation process with a home-made filtration unit.

One of the preconditions for emulsion separation was that the membrane can separate oil/water mixture selectively. Besides, the separation efficiency and separation flux values were important factors for evaluation of the membrane's performance. Therefore, we used several oil/water mixtures in order to test the oil permeation flux and separation efficiency of the PAN@LDH@OTS membrane. Figure 3d and Movie S1 (supporting information) showed the separation process for a mixture of dichloromethane (red colour) and water (blue colour) after pouring directly onto the PAN@LDH@OTS membrane surface. The oil quickly passed through the membrane,

while the water remained above it. During the separation process, the PAN@LDH@OTS membrane exhibited a fascinating permeation flux of  $6.18 \times 10^4 \text{ L m}^{-2} \text{ h}^{-1}$  and an exceptional separation efficiency of 99.973% (Figure 3c). It should be noted that there was no need of external force to facilitate the separation process. Similar experimental phenomenon can be observed for oil/water mixtures including n-hexane, toluene, petroleum ether, decane and chloroform, and the resulting permeation fluxes were  $5.51 \times 10^4$ ,  $4.20 \times 10^4$ ,  $5.13 \times 10^4$ ,  $3.15 \times 10^4$  and  $4.09 \times 10^4 \text{ L m}^{-2} \text{ h}^{-1}$ , respectively. The slight differences in the permeation fluxes can be attributed to different viscosity of the oils.<sup>22</sup> To get the purity of the separated oil, we collected the filtered oil and tested it through the Karl Fischer analyser. As shown in Figure 3d, the separation efficiency of PAN@LDH@OTS membrane for n-hexane, toluene, petroleum ether, decane and chloroform (except dichloromethane) were 99.998%, 99.991%, 99.998%, 99.999% and 99.980%, respectively. As illustrated in Table S1 (Supporting Information), the permeate flux of the PAN@LDH@OTS membrane for various oil/water mixture was higher than those reported in the literature.

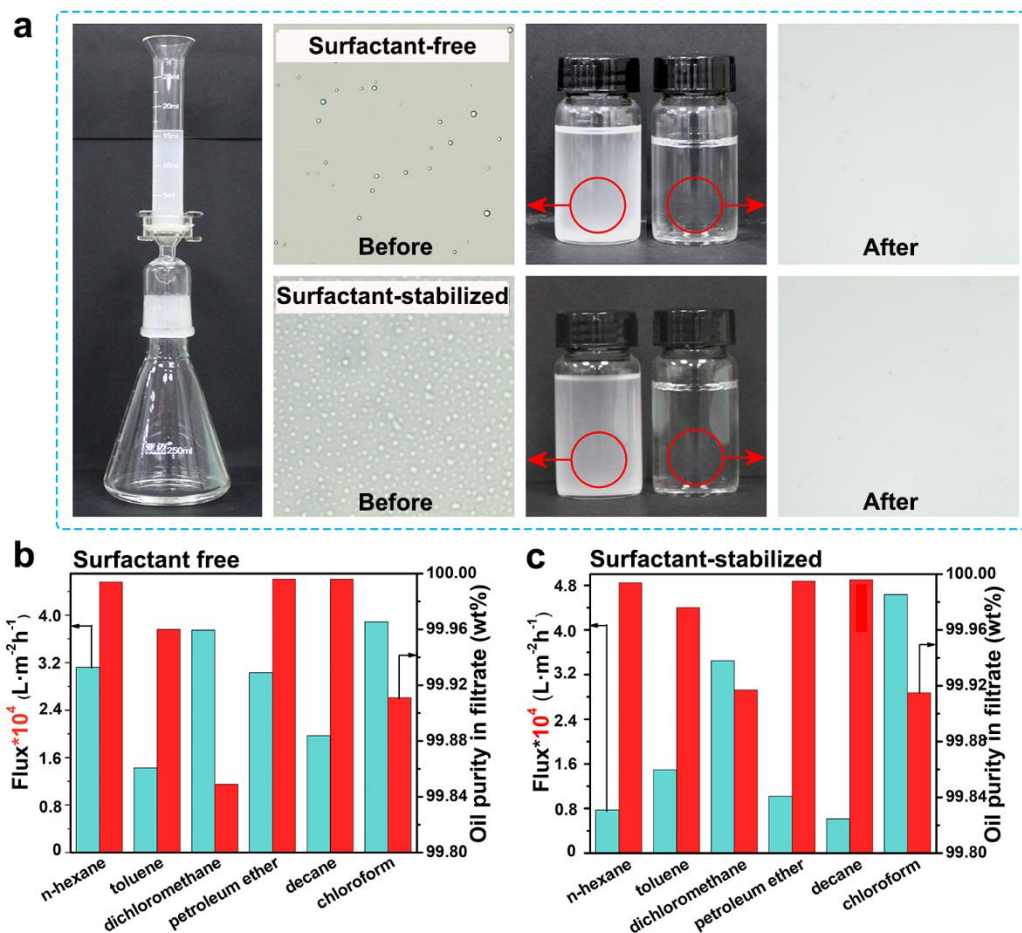


**Figure 4. Separation of SFE and SSE:** a) Separating photograph and optical microscopy images of surfactant-free and surfactant-stabilized emulsion, respectively, before and after filtration. b) SFE separation results of the PAN@LDH@OTS membrane. c) SSE separation results of the PAN@LDH@OTS membrane.

To further test the separation ability of the PAN@LDH@OTS membrane, a series of water-in-oil emulsions were prepared, which were named surfactant-free emulsion (SFE) and surfactant-stabilized emulsion (SSE), respectively. For separation of SFE, we carried out the following experiments. After a long period of time of mechanical mixing, oil and water were fully mixed, and the SFE presented a white milky state (Figure 4a and Movie S2). As shown in Figure 4b, the permeation fluxes for n-hexane, toluene, dichloromethane, petroleum ether, decane and chloroform were  $3.12 \times 10^4$ ,  $1.43 \times 10^4$ ,  $3.75 \times 10^4$ ,  $3.03 \times 10^4$ ,  $1.97 \times 10^4$ , and  $3.89 \times 10^4$   $\text{L m}^{-2} \text{h}^{-1}$ , respectively (Figure 4b). The purity of oil which calculated by measuring the water weight percentage in the filtrate after the first separation cycle was examined by using a Karl Fischer analyser.

The results indicated that the purity of all these oils were found to be above 99.84%, and some of them were up to 99.996% after the separation process, implying extremely high separation efficiency.

In the case of SSE, the Span-80 was used as surfactant to prepare the corresponding water-in-oil emulsion. For SSE, abundant tiny water droplets with diameter less than 20  $\mu\text{m}$  were observed in the photos (Figure 4a and Figure S5). When the SSE were poured onto the PAN@LDH@OTS membrane, the oil passed through the membrane immediately and water was retained on the membrane (Movie S3). During the emulsion separation process, the PAN@LDH@OTS membrane can allow oil to permeate quickly due to its superlipophilicity and to intercept the water due to the superhydrophobicity, small pore size and low surface free energy (Figure 4a). The whole process was driven solely by gravity force. Optical microscopy was used to detect the emulsion droplets and the corresponding filtrate to confirm the successful separation. Before filtration, the SSE exhibited a large number of highly dispersed oil droplets with size of  $<20\text{ }\mu\text{m}$  (Figure S5), whereas after filtration, the filtrates were transparent oil, suggesting the successful separation of the emulsion.

The slight difference in the permeation flux between SSE and SFE can be due to the difference in the viscosity of the emulsions since the flux was inversely proportional to the liquid viscosity.<sup>23</sup> For SSE, the permeation flux values fell within the range of  $4.63\times 10^4 \sim 6.16\times 10^3\text{ L m}^{-2}\text{ h}^{-1}$  (Figure 4c). It is worth noting that no external pressure was employed in the experimental set-up and the permeation process was driven solely by the gravity.

For membrane separation materials, the separation efficiency and permeation flux of the membrane were a pair of "trade off" properties. In other words, a high permeation flux was often accompanied by a low separation efficiency. In the case of the PAN@LDH@OTS membrane, it exhibited both high oil flux value ( $6.18\times 10^4\text{ L m}^{-2}\text{ h}^{-1}$ ) and high separation efficiency ( $>99.84\%$ ). Such excellent performance of the oil flux and the separation efficiency of PAN@LDH@OTS membrane demonstrated the state of the art based on the literature reports (Figure S6, Table S1). Herein, the

PAN@LDH@OTS membrane showed a promise future in the application of multifunctional oil-water separation.

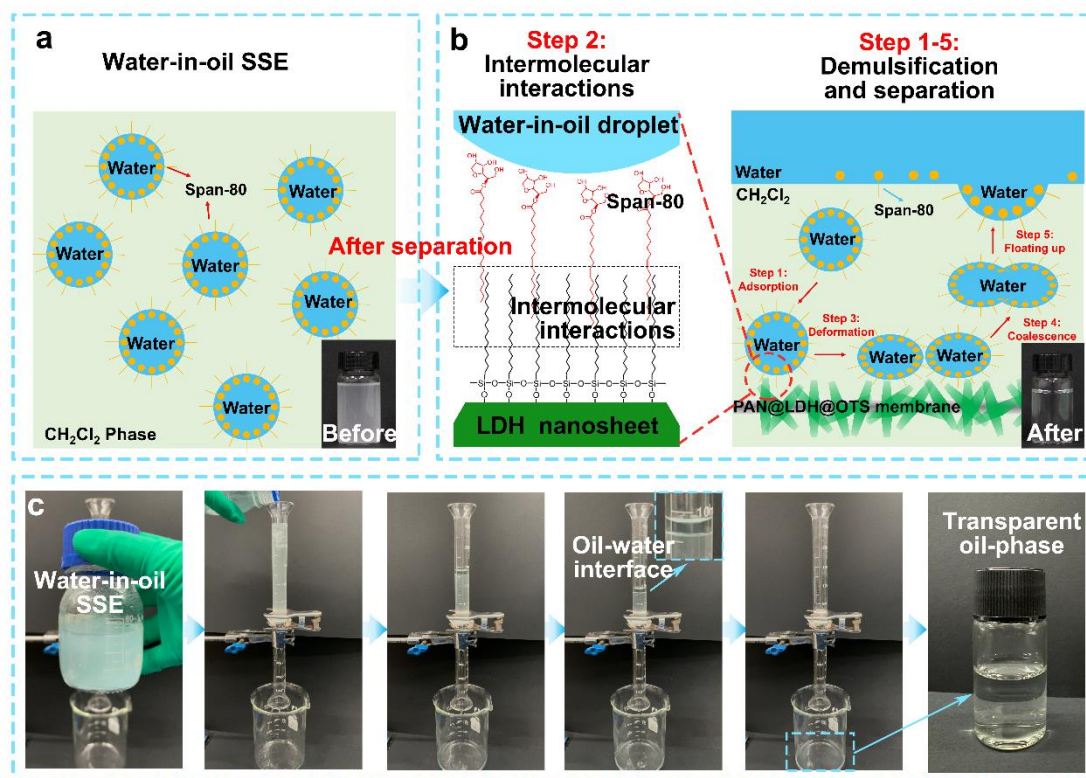


**Figure 5.** a) Schematic diagram of surfactant-stabilized water-in-oil emulsion (SSE), b) Schematic diagram of the demulsification process of SSE, c) Digital photos of SSE separation process.

From the experiments above, we summarized the separation mechanism of PAN@LDH@OTS membrane for SSE (Figure 5a-c). Initially, the SSE emulsion consisted of uniformly dispersed tiny droplets with the size  $< 20 \mu\text{m}$  (Figure 5a). Once the emulsion was poured onto the PAN@LDH@OTS membrane, oil would immediately spread and permeate through the membrane. And then, the efficient separation process can be divided into the following steps: 1) the droplets can be easily adsorbed to the membrane; 2) the stable covalent functionalization of OTS significantly reduced the surface free energy of the PAN@LDH and improved intermolecular interactions between OTS and the surfactant molecules (Span-80); 3) the droplets deformed in a second by the electropositive LDH laminate; 4-5) the deformed tiny emulsion droplets further coalesced into large droplets, floated up and finally efficient separation can be achieved. (Figure 5b).<sup>24-27</sup> The apparent deformation of water droplets



and demulsification process of SSE can be observed in Figure S7c by using Confocal laser scanning microscope (CLSM). In contrast, there was no obvious shape change of the water droplets on PAN/AlOOH and PAN@LDH membrane (Figure S7a and S7b, respectively). The SSE separation process can be clearly observed in Figure 5c, which exhibited a clear oil-water interface. Finally, the transparent and clarified oil-phase was collected. For the separation of SFE and oil/water mixture, the superlipophilicity of PAN@LDH@OTS membrane was a decisive factor to significantly improve the separation efficiency and permeation flux. In conclusion, the PAN@LDH@OTS membrane was capable of separating different type of oil-containing wastewater effectively.

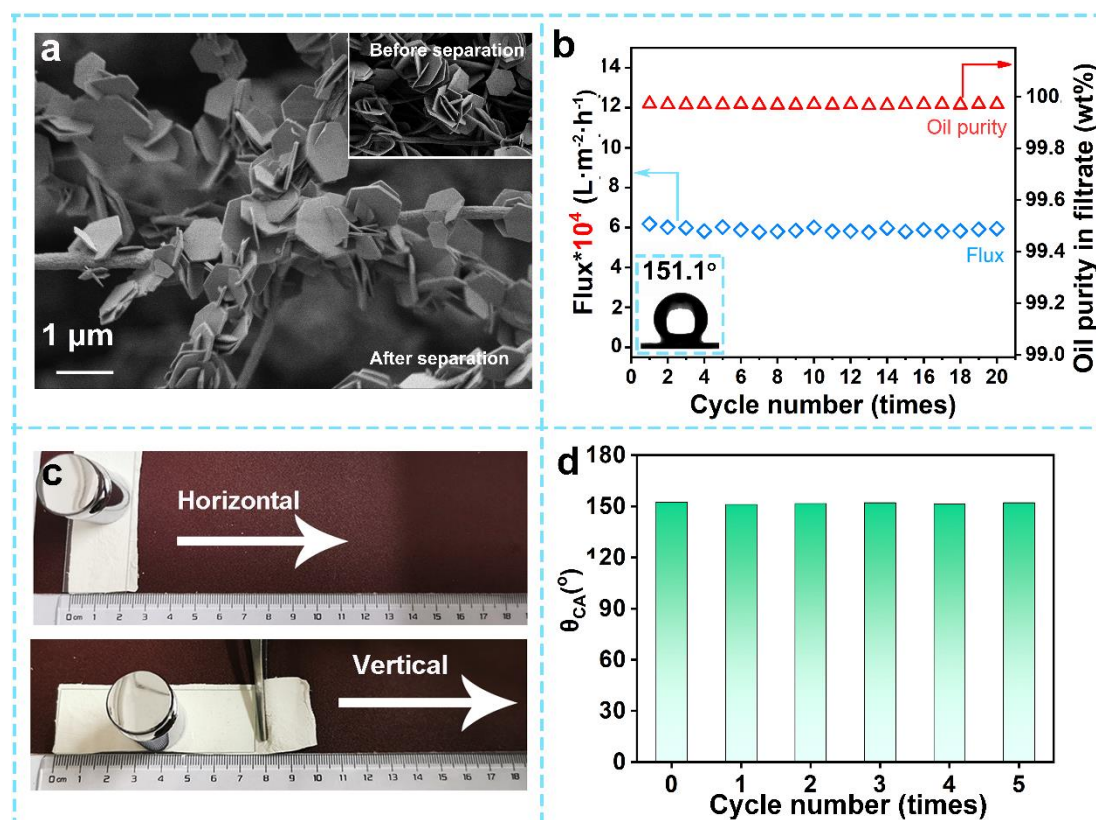


**Figure 6.** a) SEM images of PAN@LDH@OTS membrane (before and after the separation of dichloromethane/water 20 cycles); b) Recyclability of the PAN@LDH@OTS membrane for water/oil separation detected with a dichloromethane/water mixture; c) Sandpaper abrasion tests; one abrasion cycle consisted of horizontal and vertical abrasions (defined 10 cm for each direction as 1 time) by the sand paper under a weight of 100 g; d)  $\theta_{CA}$  changes after each abrasion cycle.

To test the reusability of the PAN@LDH@OTS membrane for continuous separation, the treatment of oil/water mixture was repeatedly operated. After that, the PAN@LDH@OTS membrane was washed by ethanol for 5 times and dried in oven at 60 °C for 12 h. The process was repeated for 20 cycles, and the permeation flux and separation efficiency of membrane were detected after each cycle. As shown in Figure 6b, the permeation flux decreased slightly after the 1<sup>st</sup> cycle, and kept a constant value of approximately  $5 \times 10^4 \text{ L m}^{-2} \text{ h}^{-1}$  after 20<sup>th</sup> cycles. Meanwhile, the purity of the oil can be stabilized over 99.97%. This observation suggested that the membrane retained its structural integrity and efficiency during the separation process. It can be seen from Figure 6a that SEM images of the membranes after 20 cycles showed the hydrotalcite structure was still clear. Moreover, the  $\theta_{\text{CA}}$  was not changed a lot compared with its initial value (151.1°, inset in Figure 6b), indicating the stable superhydrophobic property of the PAN@LDH@OTS membrane.

As shown in Figure 6c, in order to test the robustness of the superhydrophobic properties of PAN@LDH@OTS membrane, the sandpaper abrasion experiment was carried out.<sup>28</sup> The  $\theta_{\text{CA}}$  of PAN@LDH@OTS membrane was found to be 151.1° after 5<sup>th</sup> times of abrasion (Figure 6d), revealing that the fibrous membrane can keep the superhydrophobic properties even under harsh abrasion conditions. Also, after etching PAN@LDH@OTS membrane in 0.1 M NaOH, NaCl and HCl solution for 6 h, there were no obvious change in XRD pattern and FT-IR spectra compared with pristine PAN@LDH@OTS, indicating that the fibrous membrane can maintain chemical stability (Figure S8). The above results clearly showed that the PAN@LDH@OTS membrane possessed good durability, which was helpful to prolong the service life of membrane in actual oil-containing wastewater treatment.

## Conclusion

In summary, we reported a facile strategy to fabricate PAN@LDH@OTS membrane with the superhydrophobic/superlipophilic properties, allowing highly efficient separation of surfactant-stabilized water-in-oil emulsions (SSE). An ultrahigh



separation efficiency of >99.92% and excellent permeation flux of  $4.63 \times 10^4 \text{ L m}^{-2} \text{ h}^{-1}$  for SSE can be achieved. Detailed characterizations showed that 1) the stacked PAN fibers provided abundant pores, which was conducive to the contact between the emulsion droplets and the membrane; 2) the electropositive LDH laminate promoted the deformation of the emulsion droplets; 3) the OTS significantly reduced the surface free energy of the PAN@LDH membrane, and as a result, the inter-molecular interactions between the surfactant (Span-80) and the PAN@LDH@OTS membrane can be improved, which dramatically enhanced the demulsification process. In addition, the PAN@LDH@OTS membrane remained robust superhydrophobic properties after 5 times sandpaper abrasion test. Such superhydrophobic/superlipophilic PAN@LDH@OTS membrane showed a promising future not only in oil adsorption process, but also in various practical conditions for SFE and SSE *etc.*

## Experimental section

### Materials and Characterization

All chemicals and solvents were purchased from commercial suppliers and used without further purification. Ethanol, *N, N*-dimethylformamide (DMF), *n*-hexane, toluene, dichloromethane ( $\text{CH}_2\text{Cl}_2$ ), petroleum ether, decane and chloroform were purchased from Beijing Chemical Works.  $\text{MgCl}_2 \cdot 6\text{H}_2\text{O}$ ,  $\text{AlCl}_3 \cdot 6\text{H}_2\text{O}$  and urea were purchased from Xilong Science Co., Ltd. Oil red, methylene blue, Span-80 were purchased from Tianjin Fuchen Chemical Reagents Factory. Polyacrylonitrile (PAN,  $M_w=150000$ ) and octadecyltrichlorosilane (OTS) were purchased from J&K Scientific Co., Ltd. Deionized water (DI) was used in all reactions.

Fourier transform infrared (FT-IR) spectra were carried out on a Bruker Vector 22 infrared spectrometer using KBr pellet method. Transmission electron microscopy (TEM) images were recorded using a Hitachi H-800 instrument. TEM images were conducted on a JEOL JEM-2010 electron microscope operating at 200 kV. Scanning electron microscopy (SEM) images were obtained using a Zeiss Supra 55 SEM equipped with an EDS detector. Contact angles ( $\theta_{\text{CA}}$ ) were measured using a contact

angle meter (DSA100, Kruss), different locations were tested to provide an average value. The microscopic images of the demulsification process was observed by the confocal laser microscope (CLSM, TCSSP8, Leica). Optical microscopy images were captured by a Canon camera (600D, Japan) by dropping each water-in-oil emulsion on the calibration slide. Water-in-oil emulsion separation efficiency was measured by volumetric method Carle Fischer water meter (V20S) in Mettler Toledo Beijing Company Lab. The water contents in corresponding collected filtrates were determined using a Karl Fischer moisture titrator (C30KF Coulometer). DLS measurement was measured on a Malvern Zen 3600 (Malvern Instruments Ltd., United Kingdom).

### **Fabrication of the superhydrophobic/superlipophilic membranes**

PAN/AlOOH and PAN@LDH membranes were synthesized according to the literature.<sup>18</sup> The PAN@LDH@OTS membranes with LDH loadings of 28, 36, 47, 56 and 62% were prepared by adjusting the concentration of AlOOH in the electrospinning solution (denoted as Sample 1, 2, 3 and 4, respectively). In this study, we used 56% LDH loading on the membrane unless otherwise noted. (As shown in Figure S4)

0.001 mol of OTS and the PAN@LDH substrate were added to 150 mL of n-hexane and the reaction mixture was refluxed at 80 °C for 48 h. Upon completion of the reaction, the membrane was washed with ether and CH<sub>2</sub>Cl<sub>2</sub> and dried in an oven at 70 °C for 24 h.

**Preparation of oil/water mixtures:** Six types of **oil/water mixtures** were prepared by mixing water and oil (n-hexane, toluene, dichloromethane (CH<sub>2</sub>Cl<sub>2</sub>), petroleum ether, decane and chloroform) in 1:1 (v:v). All kinds of oil were coloured with oil red and mixed with water that was coloured with methylene blue, the relevant physical properties of the oil were indicated in Table S2

**Preparation of water-in-oil emulsions:** SFE were prepared by mixing water and oil (namely, n-hexane, toluene, dichloromethane (CH<sub>2</sub>Cl<sub>2</sub>), petroleum ether, chloroform and decane) in 1:9 (v:v) and the mixture was sonicated under a power of 2 kW for 1.5 h to produce a white and milky solution. Typically, the obtained SFE was stable within 6 h when placed in ambient conditions.

The SSE were prepared according to the literature,<sup>29</sup> which contained nanometer

size droplets. Six kinds of SSE including n-hexane, toluene, dichloromethane, petroleum ether, chloroform and decane, respectively, were prepared Typically, Span-80 (0.1 g) was added into oil (198 mL), and then water (2 mL) was added. The mixture was stirred for 3 h.

**Water-in-oil emulsion separation experiments:** The water-in-oil emulsions were separated by placing the PAN@LDH@OTS membrane between the separation devices. The separation process was only driven by gravity.

**Oil absorption experiments:** The PAN@LDH@OTS membrane was used for absorbing oil (dyed red) from oil/water (dyed blue) mixture. After each separation process, the membrane was washed with ethanol, dried and reused.

**Separation permeation flux:** The permeation fluxes of the emulsions were determined by calculating the quantity of permeate per unit time according to the following Eq. (1):

$$Flux = \frac{V}{A * t}$$

where A (m<sup>2</sup>) is the filtration surface of the membrane, V (L) is the volume of the permeate and t (h) is the separation time.

## Acknowledgments

This research was supported by the National Nature Science Foundation of China (22178019, 22208013, 22288102) and the Fundamental Research Funds for the Central Universities (XK1802-6, XK1803-05, XK1902).

## Associated content

Supporting information:

Schematic diagram of PAN@LDH@OTS membrane (Figure S1), SEM and TEM images of all membranes (Figure S2), AFM images and mean pore size of PAN@LDH@OTS membrane (Figure S3), SEM images of PAN@LDH@OTS-x% membranes, x=the loading of LDH (Figure S4), the particle size distribution of the emulsion (SSE) and filtrate (Figure S5), diagram of separation performance compared

to other works (Figure S6) CLSM images of SSE and membranes (Figure S7), and  $\theta_{CA}$  digital photos of the PAN@LDH@OTS membrane, after etching the membrane in 0.1 M NaOH, NaCl and HCl solution for 6 h (Figure S8).

## References

1. Shannon, M. A.; Bohn, P. W.; Elimelech, M.; Georgiadis, J. G.; Marinas, B. J.; Mayes, A. M., Science and Technology for Water Purification in the Coming Decades. *Nature* **2008**, *452* (7185), 301-10.
2. Gao, X.; Xu, L. P.; Xue, Z.; Feng, L.; Peng, J.; Wen, Y.; Wang, S.; Zhang, X., Dual-Scaled Porous Nitrocellulose Membranes with Underwater Superoleophobicity for Highly Efficient Oil/Water Separation. *Adv. Mater.* **2014**, *26* (11), 1771-5.
3. Cheryan, M.; Rajagopalan, N., Membrane Processing of Oily streams. Wastewater Treatment and Waste Reduction. *J. Membr. Sci.* **1998**, *151* (1), 13-28.
4. Cheng, X. Q.; Jiao, Y.; Sun, Z.; Yang, X.; Cheng, Z.; Bai, Q.; Zhang, Y.; Wang, K.; Shao, L., Constructing Scalable Superhydrophobic Membranes for Ultrafast Water-Oil Separation. *ACS Nano* **2021**, *15* (2), 3500-3508.
5. Tian, X.; Verho, T.; Ras, R. H. A., Moving Superhydrophobic Surfaces toward Real-World Applications. *Science* **2016**, *352*, 142-143.
6. Peng, C.; Chen, Z.; Tiwari, M. K., All-Organic Superhydrophobic Coatings with Mechanochemical Robustness and Liquid Impalement Resistance. *Nat. Mater.* **2018**, *17* (4), 355-360.
7. Zhao, W., Bio-Inspired Superwetable Materials: an Interview with Lei Jiang. *Nat. Sci. Rev.* **2017**, *4* (5), 781-784.
8. Darmanin, T.; Guittard, F., Superhydrophobic and Superoleophobic Properties in Nature. *Mater. Today* **2015**, *18* (5), 273-285.
9. Feng, L.; Zhang, Z.; Mai, Z.; Ma, Y.; Liu, B.; Jiang, L.; Zhu, D., A Super-Hydrophobic and Super-Oleophilic Coating Mesh Film for the Separation of Oil and Water. *Angew. Chem. Int. Ed. Engl.* **2004**, *43* (15), 2012-4.

10. Liu, J.; Wang, L.; Guo, F.; Hou, L.; Chen, Y.; Liu, J.; Wang, N.; Zhao, Y.; Jiang, L., Opposite and Complementary: A Superhydrophobic–Superhydrophilic Integrated System for High-Flux, High-Efficiency and Continuous Oil/Water Separation. *J. Mater. Chem. A* **2016**, *4* (12), 4365-4370.
11. Li, H.; Zhong, Q.; Sun, Q.; Xiang, B.; Li, J., Upcycling Waste Pine nut Shell Membrane for Highly Efficient Separation of Crude Oil-in-Water Emulsion. *Langmuir* **2022**, *38* (11), 3493-3500.
12. Wu, M.; Xiang, B.; Mu, P.; Li, J., Janus Nanofibrous Membrane With Special Micro-Nanostructure for Highly Efficient Separation of Oil–Water Emulsion. *Sep. Purif. Technol.* **2022**, *297*, 121532.
13. Zhong, Q.; Shi, G.; Sun, Q.; Mu, P.; Li, J., Robust PVA-GO-TiO<sub>2</sub> Composite Membrane for Efficient Separation Oil-in-Water Emulsions with Stable High Flux. *J. Membr. Sci.* **2021**, *640*, 119836.
14. Xu, C.; Cao, D.; Lu, W.; Sun, J.; Cheng, S., A Superhydrophobic–Superoleophilic Plasmonic Membrane for Combined Oil/Water Separation and Highly-Sensitive SERS Detection of Low Concentrations of Analytes in Oil/Water Mixtures. *New J. Chem.* **2018**, *42* (14), 11660-11664.
15. Zhang, J.; Liu, L.; Si, Y.; Yu, J.; Ding, B., Electrospun Nanofibrous Membranes: An Effective Arsenal for the Purification of Emulsified Oily Wastewater. *Adv. Funct. Mater.* **2020**, *30* (25), 2002192.
16. Lv, W.; Du, M.; Ye, W.; Zheng, Q., The Formation Mechanism of Layered Double Hydroxide Nanoscrolls by Facile Trinal-Phase Hydrothermal Treatment and Their Adsorption Properties. *J. Mater. Chem. A* **2015**, *3* (46), 23395-23402.
17. Sideris, P. J.; Nielsen, U. G.; Gan, Z.; GreyClare, P., Mg/Al Ordering in Layered Double Hydroxides Revealed by Multinuclear NMR Spectroscopy. *Science* **2008**, *321*, 113.
18. Cheng, Y.; Li, L.; He, W.; Chen, W.; Deng, G.; Song, Y.-F., Seeds Embedded Epitaxial Growth Strategy for PAN@LDH Membrane with Mortise-Tenon Structure as Efficient Adsorbent for Particulate Matter Capture. *Appl. Catal. B* **2020**, *263*, 118312.
19. Reddy, M. V.; Lien, N. T. K.; Reddy, G. C. S.; Lim, K. T.; Jeong, Y. T., Polymer Grafted Layered Double Hydroxides (LDHs-g-POEGMA): a Highly Efficient Reusable Solid Catalyst for the Synthesis of Chromene Incorporated Dihydroquinoline Derivatives under Solvent-Free Conditions. *Green Chem.* **2016**, *18* (15), 4228-4239.
20. Jung, B.; Yoon, J. K.; Kim, B.; Rhee, H.-W., Effect of Crystallization and Annealing on

- Polyacrylonitrile Membranes for Ultrafiltration. *J. Memb.Sci.* **2005**, *246* (1), 67-76.
21. Constantino, V. R. L.; Pinnavaia, T. J., Basic Properties of  $Mg^{2+i-j}Al^{3+x}$  Layered Double Hydroxides Intercalated by Carbonate, Hydroxide, Chloride, and Sulfate Anions. *Inorg. Chem.* **1995**, *34*, 883-892.
  22. Han, Z.; Li, B.; Mu, Z.; Niu, S.; Zhang, J.; Ren, L., Energy-Efficient Oil-Water Separation of Biomimetic Copper Membrane with Multiscale Hierarchical Dendritic Structures. *Small* **2017**, *13* (34), 1701121.
  23. Zhang, F.; Zhang, W. B.; Shi, Z.; Wang, D.; Jin, J.; Jiang, L., Nanowire-Haired Inorganic Membranes with Superhydrophilicity and Underwater Ultralow Adhesive Superoleophobicity for High-Efficiency Oil/Water Separation. *Adv. Mater.* **2013**, *25* (30), 4192-4198.
  24. Wu, J.; Ding, Y.; Wang, J.; Li, T.; Lin, H.; Wang, J.; Liu, F., Facile Fabrication of Nanofiber- and Micro/Nanosphere-Coordinated PVDF Membrane with Ultrahigh Permeability of Viscous Water-in-Oil Emulsions. *J. Mater. Chem. A* **2018**, *6* (16), 7014-7020.
  25. Ge, J.; Zhang, J.; Wang, F.; Li, Z.; Yu, J.; Ding, B., Superhydrophilic and Underwater Superoleophobic Nanofibrous Membrane with Hierarchical Structured Skin for Effective Oil-in-Water Emulsion Separation. *J. Mater. Chem. A* **2017**, *5* (2), 497-502.
  26. Cai, Y.; Chen, D.; Li, N.; Xu, Q.; Li, H.; He, J.; Lu, J., Nanofibrous Metal–Organic Framework Composite Membrane for Selective Efficient Oil/Water Emulsion Separation. *J. Membr. Sci.* **2017**, *543*, 10-17.
  27. Wang, X.; Yu, J.; Sun, G.; Ding, B., Electrospun Nanofibrous Materials: A Versatile Medium for Effective Oil/Water Separation. *Mater. Today* **2016**, *19* (7), 403-414.
  28. Lu, Y.; Sathasivam, S.; Song, J.; Crick, C. R.; Carmalt, C. J.; Parkin, I. P., Robust Self-Cleaning Surfaces that Function when Exposed to Either Air or Oil. *Science* **2015**, *347*, 1132-1135.
  29. Zhang, W.; Shi, Z.; Zhang, F.; Liu, X.; Jin, J.; Jiang, L., Superhydrophobic and Superoleophilic PVDF Membranes for Effective Separation of Water-in-Oil Emulsions with High Flux. *Adv. Mater.* **2013**, *25* (14), 2071-6.

# For Table of Contents Only

